AUTOMATIC PARAMETRIZATION OF GAIA ASTROMETRICALLY UNRESOLVED BINARY STARS

T.A. Kaempf[1], **P.G. Willemsen**[1], **C.A.L. Bailer-Jones**[2]

[1]Sternwarte der Universität Bonn, Auf dem Hügel 71, 53121 Bonn, Germany
[2]Max-Planck-Institut für Astronomie, Königstuhl 17, 69117 Heidelberg, Germany

ABSTRACT

We have simulated 1X photometry of spectroscopic binary stars as they will be observed by Gaia to test how well the stellar physical parameters ($T_{\rm eff_1}$, $T_{\rm eff_2}$, $\log g_1$, $\log g_2$ and [Fe/H] in addition to extinction A_V) can be determined from such unresolved objects. Both single shot (SS) and end-of-mission (EM) data was analysed and the results compared to those for single stars. We find that the parametrization performance is a strong function of the logarithmic luminosity ratio $\log(L_r)$ and also depends on the underlying grid of stellar parameter combinations. The primary star's $T_{\rm eff_1}$ and $\log g_1$ are parametrized at a similar precision as for a single star. The same applies to [Fe/H] and A_V, the two systemic parameters.

Key words: Gaia; Parametrization; Binary stars .

1. MODELLING BINARY STAR SYSTEMS

First, the two masses of a binary system are randomly drawn from a mass generating function with the secondary's mass M_2 smaller or equal to the primary's mass M_1. The mass generating function takes a random variable with uniform distribution in the range [0,1] as input and returns a stellar mass in units of the solar mass. To calculate a mass generating function based on a realistic underlying IMF, we used the equations given in Kroupa et al. (1991) and an IMF with a multi-segment power law as given in Kroupa (2001). Since the evolutionary tracks used are restrained to a mass range of 0.4 to 5 $M_\odot$, our present calculation of the IMF has only two segments with indices of $\Gamma_1 = -0.3$ for masses in the range from 0.4 to 0.5 $M_\odot$ and $\Gamma_2 = -1.3$ for 0.5 to 5 $M_\odot$. The median mass for this distribution is 0.68 $M_\odot$, while the mean mass is found to be 0.97 $M_\odot$. The corresponding temperatures for the given mass range are about 2500 and 24 000 K for Main Sequence stars, depending on [Fe/H]. In terms of spectral types this is roughly equal to a range from M8 to B2.

Next, a metallicity value for the binary system is randomly chosen from -3.3 to 0.6 dex, the range again constrained by the set of evolutionary tracks. With the masses and [Fe/H] at hand, we then interpolate in a grid of evolutionary tracks taken from Yi et al. (2003) (primordial helium abundance $Y_0 = 0.23$, helium enrichment parameter $\Delta Y/\Delta Z = 2.0$). The reason for the choice of these tracks is the high intrinsic mass and metallicity resolution of 0.1 to 0.5 $M_\odot$ and $\simeq$ 0.1 to 1.0 dex, respectively, depending on the grid location. Compared to Willemsen et al. (2004), we now use a polynomial interpolation algorithm which yields a much higher precision. For a given mass-metallicity data pair, we search the grid for the 'neighbouring' evolutionary tracks. The interpolation of the tracks is done first in terms of [Fe/H] then in terms of mass. The maximum age $age_{\rm max}$ is given by that of the heavier component, so that we can randomly choose an age for the system with the constraint that $age_{\rm system} \leq age_{\rm max}$ and $age_{\rm system} \leq age_{\rm cosmic} = 13.6$ Gyr, the currently accepted age of the universe. From the above found tracks for each $M_{\rm i}$, [Fe/H] combination we can calculate the parameters L and $T_{\rm eff}$ by doing a linear weighted interpolation between the neighbouring age values from the above obtained age of the system. The radii and $\log g$ of the components can be calculated from the temperature and luminosity. Note that the tracks used do not account for stellar evolution after the Red Giant Tip.

Having thus found the stellar parameters for each component, we linearly interpolate in the Basel2.2 grid of synthetic spectra in the order of $\log(T_{\rm eff})$, $\log g$ and [Fe/H] to find the corresponding stellar energy distributions. By randomly choosing an extinction value from the range $A_V = 0$ to 5 mag we then redden the spectra with an extinction curve from Fitzpatrick (1999) for $R = 3.1$. Note that there is only one extinction value for a physical binary system.

A spectrum of a binary system is thus defined by the parameters $T_{\rm eff_1}$, $T_{\rm eff_2}$, $\log g_1$, $\log g_2$, [Fe/H], A_V and logarithm of luminosity ratio $\log(L_r)$.

As a novelty, we introduce a rough method to simulate eclipses. Random values are chosen for parameters like separation, inclination, and phase. It is thereby determined whether there is an eclipse and additionally if it is total or partial. The components' spectra are then weighted by the stellar discs' observable areas and finally added up. We excluded binary systems in total eclipse, since these would be indistinguishable from a single star.

The simulated spectra were finally passed through the Bailer-Jones photometry simulator (Bailer-Jones 2002) to create fluxes in the MBP 1X system for magnitudes of $G = 15$ to 19 mag for 'single shot (SS)' and 'end-of-mission (EM)'.

2. PARAMETRIZATION RESULTS AND DISCUSSION

We report the parametrization results for the spectroscopic binaries as obtained from neural networks. For comparison, we also trained networks on single stars. The parameter distributions of the single stars was kept very similar to those of the binary's primary star.

The neural network code used is that of Bailer-Jones (1998). We tested both cases: end-of-mission (EM) and single shot (SS) photometry. For each magnitude, we trained a committee of 5 networks each having 11 inputs from the 1X photometry, two hidden layers (both made up of 15 neurons), and seven output parameters, namely $T_{\rm eff_1}$, $T_{\rm eff_2}$, $\log g_1$, $\log g_2$, [Fe/H], A_V and the logarithm of the luminosity ratio $\log(L_r)$. In the case of single stars there are naturally only four parameters. If not stated otherwise, we report the average (over some set of spectra) errors for each parameter, i.e.,

$$A = \frac{1}{N} \cdot \sum_{p=1}^{N} |C(p) - T(p)| \qquad (1)$$

where p denotes the $p^{\rm th}$ star (or rather its fluxes in the different filters) and T is the target (or 'true') value for this parameter. The quantity $C(p)$ here is the classification output averaged over the committee of 5 networks. Note that the networks were trained on the complete training set. Only for the analysis, the validation set was split into certain parameter ranges, i.e., we did not use specialised networks for training.

The overall parametrization results are shown in Figure 1 for EM and SS photometry. From the temperature and gravity results we immediately see that the errors of the secondary are very large for the temperature and very small for the gravity determination. Inspection of Table 1 shows that the errors for both parameters of the secondary are close to random; the results are much biased due to the non-uniform distribution of secondaries in the parameter space. The small range of allowed values for these parameters will almost always result in a good estimation (even for untrained networks). However, inspection of the parameter estimates for the complete system (extinction A_V and metallicity [Fe/H]) and the primary component ($T_{\rm eff_1}$, $\log g_1$) shows that the networks really converged: the errors are below those of random networks.

From Figure 1 we also see that the parameter determinations of the primary and those of the whole system ([Fe/H] and A_V) are not much affected by the presence of a second star, when compared to the results for single stars. Though this is probably somehow due to the non-uniform distribution of the secondary, we would have

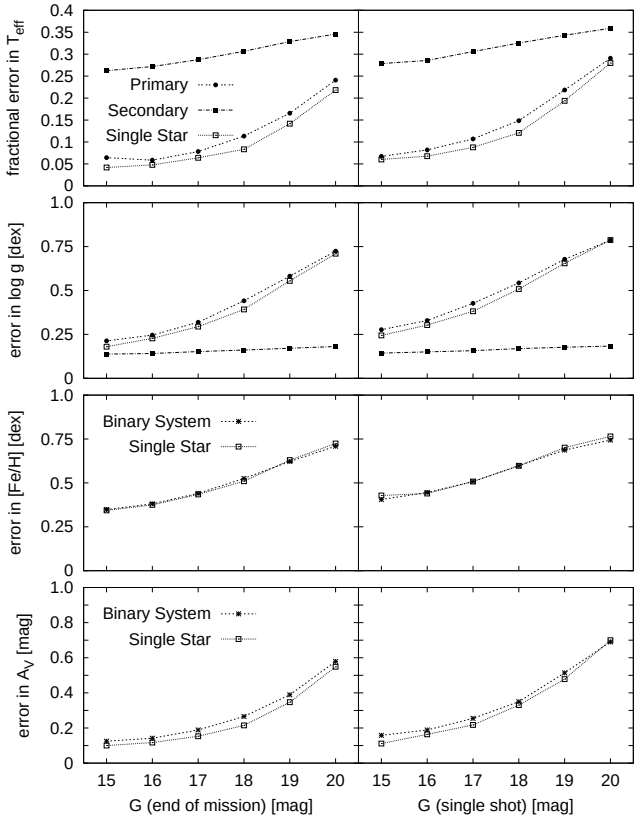

Figure 1. The parametrization results for end-of-mission (left column) and single shot (right column) photometry for the two components' temperatures (top), gravities (second row) and the system's metallicity and extinction. Note that there is only one metallicity and extinction value for the spectroscopic binary system. The error is that of Equation 1. The temperature errors are fractional errors. Note that the non-uniform parameter distribution of the secondary yields under- and over-estimated results for the temperature and gravity, respectively.

expected a stronger decline for those parameters which strongly affect the continuum of a spectrum ($T_{\rm eff}$ and A_V).

The differences in the appearance of the error curves for EM and SS photometry are small. In general, line sensitive parameters like [Fe/H] and $\log g$ are more affected by declining S/N than parameters which primarily change the continuum ($T_{\rm eff}$ and A_V). This is what one expects from the signals and what was found in earlier studies (see e.g., Brown 2003).

3. THE DEPENDENCE OF PARAMETRIZATION ON $T_{\rm EFF}$ AND LOG($L_{\rm R}$

In this section we examine the parametrization results for certain ranges of the first component's temperature $T_{\rm eff_1}$ and the overall logarithmic luminosity ratio $\log(L_r)$. Figure 2 (EM) shows the mean and standard deviation of the difference *computed*($T_{\rm eff}$) – *true*($T_{\rm eff}$) as a function of logarithmic luminosity ratio for the complete sample

Table 1. Parametrization results for networks trained on grids of binaries. Left column for a network trained on data without noise, right column for a random (untrained) network.

Parameter	error (no noise)	error (random)
$T_{\rm eff_1}$[%]	4.1	49.5
$T_{\rm eff_2}$[%]	25.9	36.3
$\log g_1$[dex]	0.175	1.093
$\log g_2$[dex]	0.127	0.238
[Fe/H][dex]	0.238	0.789
A_V[mag]	0.095	1.256

and for the validation set split in two temperature ranges of the first component. The corresponding result for the gravities is shown in Figure 3 (EM) while those for metallicity and extinction are presented in Figure 4 (EM).

From Figure 2 we see that there are strong systematic deviations of the secondary's temperature estimates. For small values of $\log(L_r)$ the secondary's temperature is strongly underestimated while for higher $\log(L_r)$ there is an overestimation. This is certainly due to the distribution of the secondary's parameters. Interestingly, we see that for those binaries where the first component has lower temperatures ($T_{\rm eff_1} \leq 10\,000$ K), the temperature determination of the secondary works rather well. This is most probably due to the presence of Red Giants at low temperatures. There are thus many RG-MS and RG-RG combinations, while for higher temperatures ($T_{\rm eff_1} > 10\,000$ K) we expect a larger fraction of MS-MS combinations. Of course, two rather different stars (RG and MS) in a system are easier to identify as a binary (if the MS stars is sufficiently hot) than two very similar stars. We would therefore expect that the temperature of the second component is better estimated for lower temperatures of the first component. Note that the secondary's temperature error curves are very similar for $T_{\rm eff_1} > 10\,000$ K for different magnitudes (i.e., independent of S/N) while those for $T_{\rm eff_1} \leq 10\,000$ K have a clear dependence on S/N. This is strong evidence that the parametrization of the secondary is not random at least for the latter case.

From Figure 2 for the first component, we find that binaries with a high temperature primary ($T_{\rm eff_1} > 10\,000$ K) generally have larger standard deviations (of the difference *computed – true*) than those objects were $T_{\rm eff_1} \leq 10\,000$ K. This may be at least partly explained by the larger steps in temperature for hotter objects.

The dependence of the temperature determination for the primary on the luminosity ratio is very similar to what Weaver (2000) found for spectral types. The same can be said for $\log g$ shown in Figure 3: the errors are largest for small luminosity ratios and then decrease smoothly until remaining almost constant as $\log(L_r)$ increases. This was also found by Weaver (2000) albeit for luminosity classes. A too-low luminosity ratio has a stronger effect on the parametrization than a very high ratio. It seems that there is a lower limit for $\log(L_r)$ for which the components' parameters can be well determined. While Weaver (2000) found almost similar spectral type and luminosity class errors for the cooler and hotter companion (in fact, the luminosity errors are even lower for the cooler star), our results are certainly biased due to the underlying grid of parameters. Actually, we also expect the results of Weaver (2000) to be biased, but in a different way due to different parameter distributions.

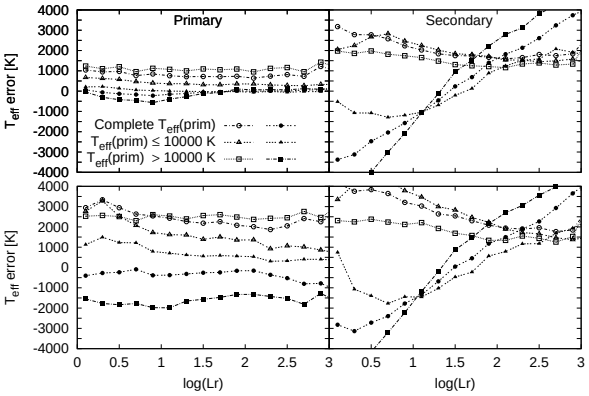

Figure 2. The mean (filled symbols) and standard deviation (open symbols) of the difference computed($T_{\rm eff}$) – true($T_{\rm eff}$) as a function of log(L_r) for $G_{\rm EM} = 15$ mag (top) $G_{\rm EM} = 19$ mag (bottom).

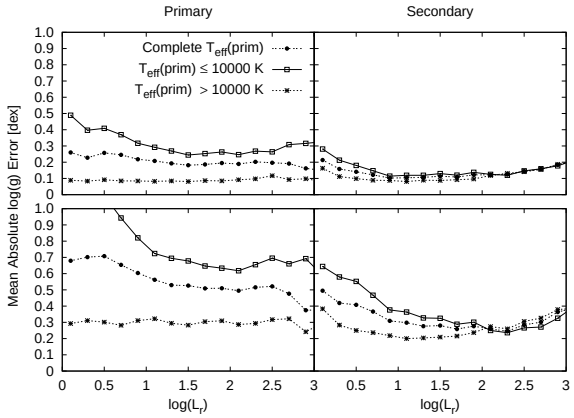

Figure 3. The errors of gravity as a function of log(L_r) for $G_{\rm EM} = 15$ (top) and 19 mag (bottom). Due to the second component's non-uniform parameter distribution (many MS stars), the estimated $\log g_2$ errors are too optimistic.

For gravity we find for both components that this parameter can be better determined for higher temperatures. This is qualitatively in agreement with the parametrization results for single stars (see e.g., Brown 2003). The high fraction of Red Giants in our test set is supposed to deteriorate the results for low temperature objects since especially stars with temperatures near 5000 K show larger errors (on average) for $\log g$ than at other temperatures (see e.g., the results of Kaempf & Willemsen in Brown 2003). The dependence of the $\log g$ errors on temperature (at least for $\log(L_r) \leq 2$) is again evidence for a non-random parametrization of this component.

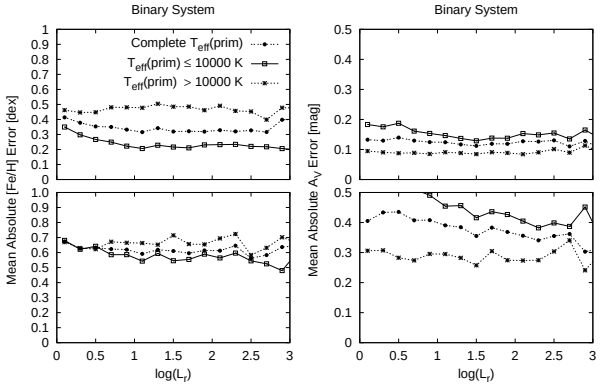

Figure 4. The errors of metallicity [Fe/H] (left column) and extinction A_V (right column) as a function of log(L_r) for $G_{\rm EM} = 15$ mag (top) and $G_{\rm EM} = 19$ mag (bottom).

As can be seen from Figure 1, the parametrization results for [Fe/H] and A_V of the binary system are very similar to that of single stars. The errors in Figure 4 do not show strong dependencies of log(L_r). Note however the slight increase of the metallicity error for lower luminosity ratios – similar to what is seen for temperature and gravity errors. Naturally, the parametrization of metallicity works better for low temperature objects while that of extinction yields smaller errors at high temperatures (this distinction is only for the temperature of the primary, but since $M_2 \leq M_1$ we assume that the first component dominates the spectrum). For $G_{\rm EM} = 15$ mag (complete temperature range) we find that [Fe/H] can be determined to better than 0.4 dex for all luminosity ratios and for cool primaries ($T_{\rm eff_1} \leq 10\,000$ K) even to $\simeq 0.25$ dex for log(L_r) ≥ 1. For fainter objects the errors quickly increase until at $G_{\rm EM} = 19$ mag the estimated metallicity values are almost random for all log(L_r).

Extinction can be determined to better than $\simeq 0.14$ mag for the complete temperature range at $G_{\rm EM} = 15$ mag (Figure 4). Increasing the magnitude from $G_{\rm EM} = 15$ mag to 19 mag again results in larger errors (from 0.13 mag to 0.44 mag at log(L_r)=0.5 and 0.11 mag to 0.37 mag at log(L_r)=1.5). Also, binaries with a cool primary seem to be more difficult to probe for A_V than those with a hotter primary. However, unlike with [Fe/H] we are certainly not approaching random values.

4. CONCLUSIONS

We conclude that the parametrization performance as a function of S/N and log(L_r) behaves similar to that of the classification problem (Willemsen et al. 2005). The parameters of binaries with low luminosity ratios log(L_r) ≤ 0.5 are generally harder to estimate than for higher ratios. Indeed, it seems the best results can be obtained for log(L_r) ≥ 1, but a too-high log(L_r) again deteriorates the results. The results also emphasise that the underlying distribution of the parameters has a strong influence on the parameter estimates. The overall parametrization results for the first component are similar albeit a little worse as compared to single stars. This is understandable as the parameter degeneracy, i.e., the fact that different parameters can have the same influence on the stellar energy distribution, is naturally larger for binary systems. The errors for the second component are generally larger than those of the first. For systems with $T_{\rm eff_1} \leq 10\,000$ K (a larger fraction of RG-MS or SGB-MS combinations) we find fractional temperature errors of $\simeq 7\%$ and 20% for the primary and secondary component at log(L_r)=1 for $G_{\rm EM} = 15$ mag. These increase to 20 and 30% at $G_{\rm EM} = 19$ mag. As for single stars, line sensitive parameters are more affected by lower S/N. However, a determination of $\log g_1$ to better than ~ 0.6 for log(L_r) ≥ 1 at $G_{\rm EM} = 19$ mag is possible. The results show further that the determinations of the system's parameters, i.e., metallicity [Fe/H] and extinction A_V are not much affected by the presence of another component. See Willemsen et al. (2004) for more on the topic.

REFERENCES

Bailer-Jones, C.A.L. 1998, Statnet - a feedforward interpolation neural network, Technical report, see http://www.mpia-hd.mpg.de/homes/calj/statnet.html

Bailer-Jones, C.A.L. 2002, Gaia techical report ICAP-CBJ-004

Brown, A. 2003, Gaia techical report ICAP-AB-004

Fitzpatrick, E. L. 1999, PASP, 111, 63

Kroupa, P., Gilmore, G., & Tout, C. A. 1991, MNRAS, 251, 293

Kroupa, P. 2001, MNRAS, 322, 231

Weaver, W. 2000, ApJ, 541, 298

Willemsen, P., Kaempf, T., & Bailer-Jones, C. A. L. 2004, Gaia techical report ICAP-PW-003

Willemsen, P., Kaempf, T., Bailer-Jones, C.A.L., de Boer, K., 2005, ESA SP-576, this volume

Yi, S. K., Kim, Y., & Demarque, P. 2003, ApJS, 144, 259